

# THERMODYNAMIC ASPECTS OF DROSS GENERATION

Jinichiro Nakano<sup>1</sup>, Gary R. Purdy<sup>2</sup> and Dmitri V. Malakhov<sup>2</sup>

<sup>1</sup> Department of Materials Science and Engineering, Carnegie Mellon University, 5000 Forbes Avenue  
Pittsburgh, Pennsylvania, USA 15213

<sup>2</sup> Department of Materials Science and Engineering, McMaster University  
1280 Main Street West, Hamilton, Ontario, Canada L8S 4L7

## ABSTRACT

Thermodynamics alone is insufficient for the in-depth understanding and quantitative modeling of the processes accompanying galvanizing and galvannealing. It must be coupled with kinetics of nucleation and growth of intermetallic phases, both on the surface of the steel strip continuously fed into the bath (resulting in a desired protective coating) and in the bath (resulting in unwanted dross). The analysis in this contribution is based on two assumptions. Firstly, on contact with the bath, the solubility of iron is governed by a metastable equilibrium quickly established between the liquid and BCC phases. A volume of liquid supersaturated with Fe, continuously forming near the immersion point, is then dissipated by, *e.g.*, flows in the bath. The second conjecture is that the melt reduces this supersaturation by forming intermetallic phases. From isonucleation diagrams calculated by means of a newly developed Zn–Fe–Al database, variations in temperature and aluminum content show a pronounced effect on the probable nature of phases appearing in the system.

Keywords: galvanizing, galvannealing, dross formation, thermodynamics, zinc bath management,

## INTRODUCTION

In continuous hot-dip galvanizing lines, steel strips are introduced at high velocity in a liquid Zn bath containing small additions of Al at temperatures 450–470°C. During the dipping process, isolated intermetallic particles (dross) also form in the bath, causing numerous problems such as quality degradation of the coatings, and economic and environmental problems. Such by-products normally consist of Al-bearing Zn–Fe based phases ( $\zeta$  and  $\delta$ ) and/or of Zn-bearing Fe–Al based phases ( $\text{Fe}_2\text{Al}_5$ ), depending mainly on the bath temperature and chemistry. Intermediate phases in the Zn–Fe–Al system are presented in Table 1 along with their sublattice models<sup>1)</sup>.

Table 1: Sublattice models of intermediate phases<sup>1)</sup>

Phase	Sublattice model
$\zeta$	$(\text{Fe}, \text{Va})_{0.072} (\text{Al}, \text{Zn}, \text{Va})_{0.072} (\text{Zn})_{0.856}$
$\delta$	$(\text{Fe})_{0.058} (\text{Al}, \text{Fe}, \text{Zn})_{0.180} (\text{Zn})_{0.525} (\text{Zn})_{0.237}$
$\Gamma$	$(\text{Fe}, \text{Zn})_{0.154} (\text{Fe}, \text{Zn})_{0.154} (\text{Al}, \text{Fe}, \text{Zn})_{0.231} (\text{Zn})_{0.461}$
$\Gamma_1$	$(\text{Fe})_{0.137} (\text{Al}, \text{Fe}, \text{Zn})_{0.118} (\text{Zn})_{0.745}$
$\Gamma_2$	$(\text{Al}, \text{Fe}, \text{Zn})_{0.255} (\text{Zn})_{0.745}$
$\text{Fe}_4\text{Al}_{13}$	$(\text{Al})_{0.6275} (\text{Fe}, \text{Zn})_{0.235} (\text{Al}, \text{Zn}, \text{Va})_{0.1375}$
$\text{Fe}_2\text{Al}_5$	$(\text{Fe})_2 (\text{Al})_5 (\text{Zn}, \text{Va})_3$
$\text{FeAl}_2$	$(\text{Fe})_1 (\text{Al})_2 (\text{Zn}, \text{Va})_{0.035}$
$\text{Fe}_4\text{Al}_5$	$(\text{Al}, \text{Fe})_1$

Assuming the existence of a metastable equilibrium between pure Fe and liquid, rigorous kinetic modeling of Fe dissolution was performed by Giorgi *et al.*<sup>2)</sup>. In their work, some of the dissolved Fe is assumed to return to the substrate to aid the formation of coating whereas the remainder is presumed to contribute to the precipitation of dross particles in the bath. Supersaturation in the immediate vicinity must be reduced to some extent. Ajersch *et al.*<sup>3)</sup> simulated dross formation by utilizing a numerical model incorporating fluid flow and mass transport in the bath. It was assumed that dross nucleates whenever and wherever equilibrium is disturbed to cause supersaturation. Both models by Giorgi *et al.* and Ajersch *et al.* can be validated if the potential dross phases, corresponding to different degrees of supersaturation, are known.

Our thermodynamic conjecture is based on supersaturation created by an excess amount of Fe dissolved into the bath in order to attain the metastable BCC-liquid local equilibrium. The concept of a metastable solid-liquid equilibrium has frequently been introduced to explain the substantial amount of iron found in the bath<sup>4-10</sup>. This assumes that the steel-bath interface rapidly experiences a local metastable equilibrium on first contact, and that Fe is transported away from the steel strip into the bath until more stable equilibria are established, due to the nucleation and growth of intermediate Zn-Fe-Al phases. Much of the dissolved Fe will circulate within the bath until it encounters more favourable nucleation or growth sites such as dross particles (including oxides), at which time it can combine with Zn and Al to promote the growth of the particle. The potential degree of supersaturation increases at a much higher rate with decreasing Al content of the bath, whereas increasing the bath temperature has a negative impact on supersaturation<sup>10</sup>. It is therefore difficult to predict which stable dross phases will nucleate from the bulk bath composition as they form at any time or location in the bath.

An isothermal section of the Zn-Fe-Al system at 450°C shown in Figure 1 was calculated using a recently developed thermodynamic model<sup>1</sup>. This ternary system is known to possess a true ternary phase ( $\Gamma_2$ ) near the  $\delta$  phase composition; however, the ternary phase occurs only after a long homogenization<sup>11-13</sup>. Thus, the  $\Gamma_2$  dross particles are not commonly observed in industrial baths (except for some locations where a long equilibration is possible)<sup>14</sup>. This phase features a very similar X-ray diffraction pattern to  $\delta$ <sup>15,16</sup> and  $\Gamma_1$ <sup>11</sup>, a property that may mislead a researcher.

Phase equilibria in galvanizing liquid are also strongly affected by temperature. In this contribution, this variation is visited by comparing computed equilibria with experimental findings. Furthermore, computed driving forces for the onset of precipitation are utilized to discuss the possibility of formation of different metastable dross and coating phases, a question that cannot be clarified solely by the phase diagram approach.

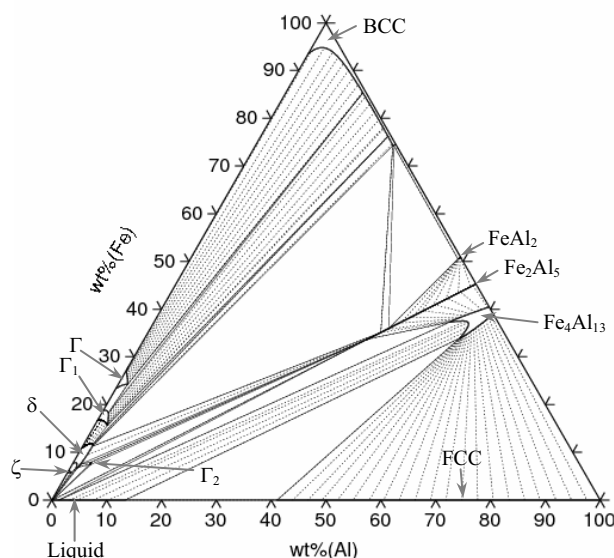


Figure 1: A computed isothermal section of the Zn-Fe-Al system at 450°C<sup>1</sup>

## THERMODYNAMIC CONSIDERATIONS

### Temperature Dependence of Phase Equilibria

Zn-rich corners of isothermal sections of the Zn-Fe-Al system at temperatures of 420°C, 450°C and 480°C are shown in Figure 2. Among all the phase diagram evaluations previously reported for the Zn-Fe-Al system, only three of them – Perrot *et al.*, Yamaguchi and Tang *et al.*<sup>11-13</sup> – reported the ternary phase  $\Gamma_2$  at the zinc-rich corner, utilizing long equilibration times, 1000 hours, 1000 hours and 360 hours, respectively. In order to show a full equilibrium system, this ternary phase is included in Figure 2, although it does not normally appear in general galvanizing practice. A metastable phase diagram is shown in Figure 2-d, where the  $\Gamma_2$  phase is suppressed.

At 450°C (Figure 2-b), the  $\zeta$ ,  $\delta$  and  $\Gamma_2$  phases are all in equilibrium with liquid<sup>11-13</sup>. It is interesting to note that  $\delta$  can be in equilibrium with six phases (BCC, liquid,  $\zeta$ ,  $\Gamma_1$ ,  $\Gamma_2$  and  $\text{Fe}_2\text{Al}_5$ ) at the same time at this temperature.  $\delta$ , however, loses its contact with BCC and liquid at temperatures close to the Zn melting point (419°C), which is supported by

Yamaguchi's experimental finding<sup>17)</sup> that the  $\delta$  phase was no longer in equilibrium with liquid at 425°C (Figure 2-a). Instead,  $\Gamma_2$  was equilibrated with  $\zeta$  to form a three-phase equilibrium with liquid.

The computed stability region of the  $\Gamma_2$  phase contracts with increasing temperature and completely disappears as temperature is raised beyond 465°C<sup>17)</sup> (Figure 2-c).  $\delta$  and  $\Gamma$  expand their homogeneity regions with temperature whereas  $\Gamma_1$  becomes less stable at higher temperatures. This can be also deduced from the binary Zn-Fe system<sup>18)</sup>.

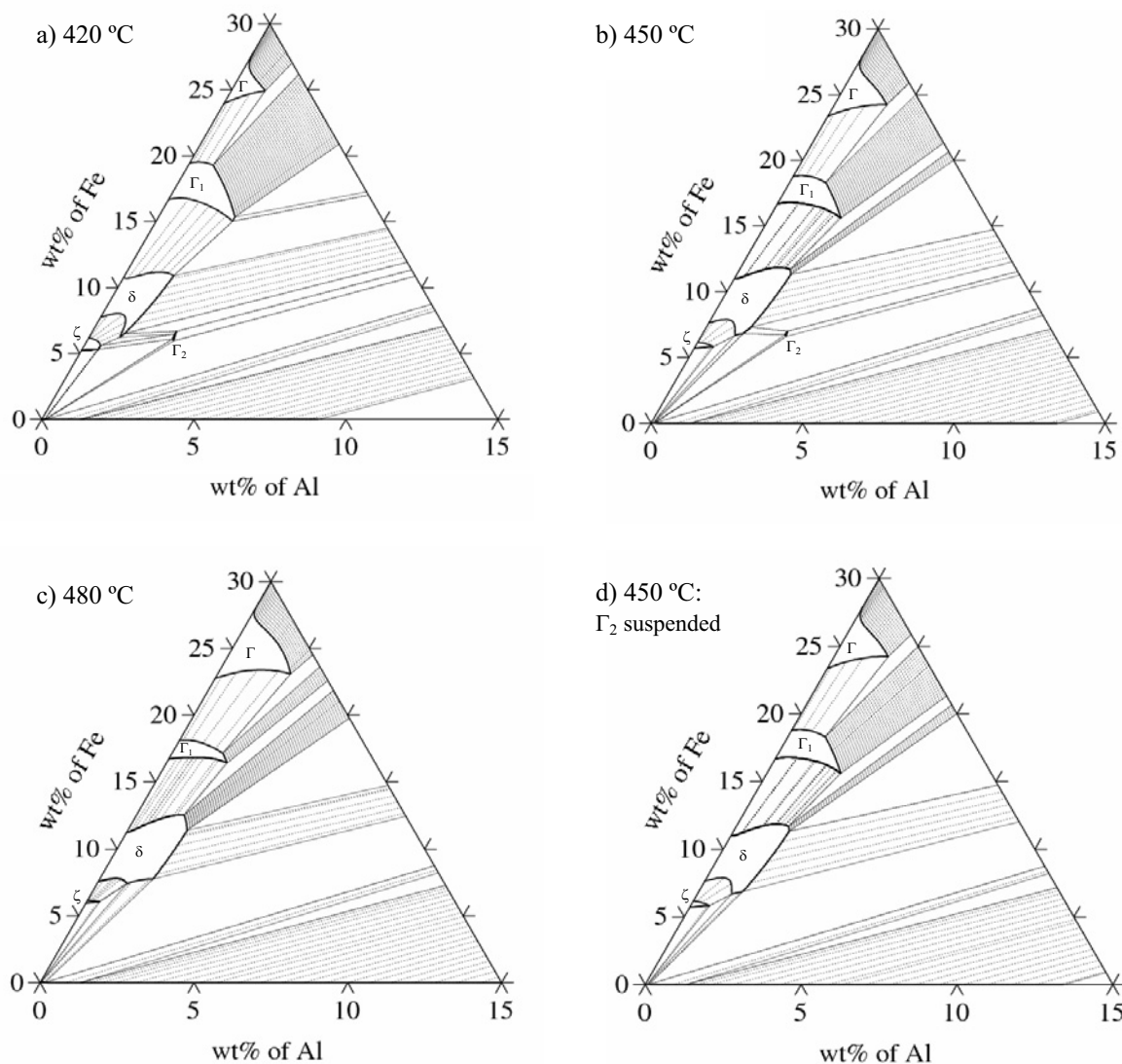


Figure 2: Calculated global phase equilibria at a) 420°C, b) 450°C, c) 480°C and d) 450 °C (Note:  $\Gamma_2$  is suppressed in d))

### The Metastable $\delta$ Phase

If, due to kinetic reasons, the  $\delta$  phase nucleates from the metastable BCC-liquid mixture, its homogeneity region is largely extended since there are no other phases competing with  $\delta$  and affecting its phase boundaries. Two- and three-phase equilibria among BCC, liquid and  $\delta$  phases at 450°C are shown in Figure 3. Perrot *et al.*<sup>11)</sup> reported an extended homogeneity region of the metastable  $\delta$  phase, utilizing a short-equilibration experiment (30 minutes). As Figure 3 indicates, their result (dashed curve) is in an agreement with the calculated homogeneity contour.

When the system tends to a global equilibrium, the homogeneity range of the  $\delta$  phase narrows until it finally coincides with the equilibrium one. The remaining supersaturation in the  $\delta$  phase may be spent on the formation of new phase(s). For example, if at a certain Al content, supersaturated liquid is somehow trapped inside this  $\delta$  particle, the  $\Gamma_2$  phase may nucleate in the liquid and grow by a liquid film migration mechanism<sup>19)</sup>.

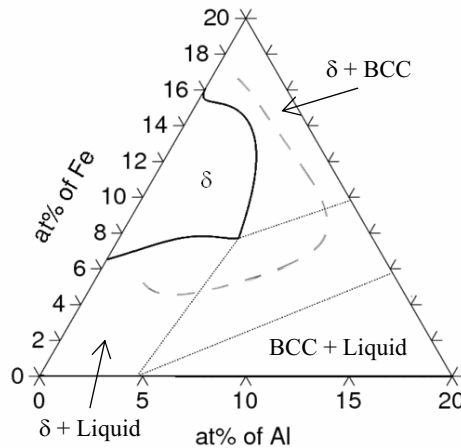


Figure 3: A computed metastable homogeneity region of  $\delta$  at 450°C (dashed: experimental<sup>11)</sup>)

**Driving Forces for the Dross formation**

The driving force discussed here is a measure of the potential for nucleation of a phase from a supersaturated parent phase; it must be distinguished from the driving force for the complete precipitation reaction, determined by the difference between the free energy of the parental phase and a common tangent at an alloy composition. The presence of metastable phases may often be rationalized in terms of the driving force for nucleation.

Details of calculation of the driving force for the onset of precipitation were discussed by Purdy *et al.*<sup>20)</sup> who applied the concept developed by Hillert<sup>21)</sup> to compute “isonucleation” diagrams in multicomponent systems. The driving force for the onset of precipitation is equal to the maximal difference in chemical potentials of a component between the matrix and the forming phase. For example, the driving force of the beginning of the  $\delta$  phase from a supersaturated binary Zn–Fe liquid phase can be expressed as

$$-\Delta G_m^\delta = G_{(w\% \text{ in LIQ})}^{\text{LIQ}} + \frac{\partial G^{\text{LIQ}}}{\partial x^{\text{LIQ}}} (x^\delta - x^{\text{LIQ}}) - G_{(w\% \text{ in } \delta)}^\delta$$

whose value indicates the possibility of nucleation of  $\delta$  if it is positive. A graphical representation corresponding to equation 1 is shown in (Figure 4). In the case where a plurality of phases are possible candidates, and where no significant differences in interfacial free energy exist, the phase with the highest driving force would be considered to be the one that first nucleates from the supersaturated liquid phase. In Figure 4, a tangent between BCC and liquid is drawn so as to indicate this  $\delta$  is forming from liquid supersaturated at the solubility limit during galvanizing processes.

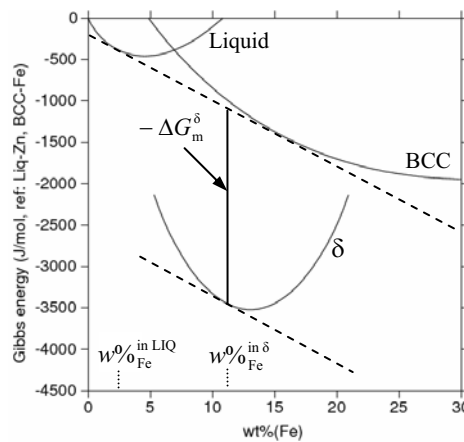


Figure 4: A double-tangent construction for calculating driving force of nucleation

Under the assumption of local equilibrium, the interface supposedly reaches the maximum Fe solubility on immersion in the bath. However, the amount of Fe in solution in the liquid (and the corresponding nucleation potential) will fall away with increasing distance from the strip.

The phase with the highest driving force varies with composition at fixed temperature. Boundaries can therefore be drawn to delineate a region of energetic preference for the formation of each phase from supersaturated solution.

Figure 5 shows such domains (dotted), superimposed onto the isothermal section of the Zn–Fe–Al system at 450°C (black solid). Note that the  $\Gamma_2$  phase is suspended here for practical purposes. Isodriving force contours (gray solid) are shown for the phase with the highest driving force. If the bath Al content is known, then the phase with the greatest driving force for nucleation can be deduced from the degree of supersaturation with Fe (dashed). It is interesting to note that, at lower Al concentrations, driving forces of nucleation in the immediate vicinity of the interface become smaller even though the maximal Fe solubility is higher.

The  $\delta$  phase holds the most potential even in the  $\zeta$ +liquid phase region if iron solubility slightly exceeds the equilibrium value. It is also true for  $\text{Fe}_2\text{Al}_5$  in the  $\delta$ +liquid region.  $\text{Fe}_2\text{Al}_5$  is in fact, for a typical galvanizing composition, a phase likely to nucleate first from the supersaturated interface or bath as dictated by the upper limit of Fe dissolution. This is postulated for the interface or the immediate vicinity. For other locations away from the interface, the much less Fe supersaturation must be considered but domains of the highest driving force can be still estimated by using the same isonucleation diagram.

This diagram may also be relevant to alloy formation in coatings as galvanizing layers form at the interface. Under the local equilibrium assumption, the steel-bath interface in a continuous hot-dip galvanizing bath is always supersaturated with Fe on the initial immersion. Figure 5 implies that the metastable  $\text{Fe}_2\text{Al}_5$  phase (inhibition layers) would nucleate at the supersaturated interface even in the  $\delta$ +liquid region. However, coating formation is also strongly affected by surface topology and the availability of Fe.

It must be noted that the driving forces are all negative in the liquid homogeneity region because the liquid phase has the lowest Gibbs energy there. The global liquidus curve therefore corresponds to the isodriving force of zero. The driving force should be treated carefully since it does not take into account the important factors of surface energies of intermetallics and kinetics of their formation.

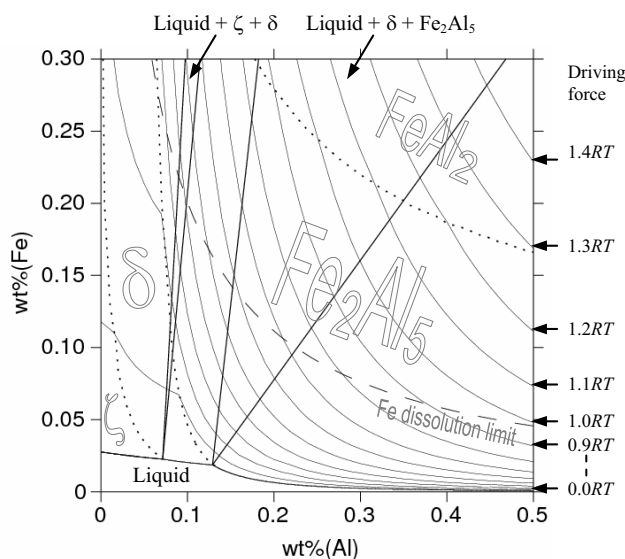


Figure 5: Isonucleation diagram superimposed on the isothermal section of Zn–Fe–Al at 450°C

## CONCLUSION

By invoking thermodynamic argumentation, an influence of temperature and aluminum concentration on the nature and amount of dross particles forming during galvanizing and galvannealing of steels is revealed. In particular, it is demonstrated that  $\text{Fe}_2\text{Al}_5$  dominates within a wide range of temperatures and Al concentrations, but that  $\zeta$ ,  $\delta$  and  $\text{FeAl}_2$  intermetallics can also form for temperatures and concentrations encountered in practice.

All quantitative estimations become possible due to a recently developed exhaustive thermodynamic model of the Zn–Fe–Al system (a corresponding Thermo-Calc compatible database is available upon request). In particular, computational thermodynamics predicts that the ternary  $\Gamma_2$  phase becomes unstable at temperatures exceeding 480°C, which is in an excellent agreement with experimental observations. It can also be employed for understanding why the

homogeneity region of the  $\delta$  phase is affected so dramatically when the formation of other intermetallics is kinetically impeded.

The computations are based upon the critical assumption that iron dissolves very rapidly when it is brought into contact with molten zinc, and that its solubility limit is dictated by a metastable equilibrium between the liquid and BCC phases. A subsequent dissipation of this Fe-rich volume of melt by transport processes within the bath results in the supersaturation of the liquid phase with iron. It is assumed that this supersaturation is relieved by nucleation and growth of dross particles. It is hypothesized that an intermetallic phase possessing the largest driving force for the onset of precipitation is the one most likely to form. By using these conjectures, it is demonstrated that temperature and Al concentration perceptibly affect the magnitude of the driving forces, *i.e.* the nature of dross particles continuously forming within a supersaturated melt.

#### ACKNOWLEDGEMENT

The authors gratefully acknowledge the support of the Natural Sciences and Engineering Research Council of Canada and the McMaster Steel Research Centre.

#### REFERENCES

- 1) J. Nakano, D. V. Malakhov, S. Yamaguchi, G. R. Purdy, *CALPHAD*, **31** (2007): 125-140
- 2) Giorgi, M. -L., Guillot, J. -B., Nicolle, R. in: Galvatech 2004: 703-711
- 3) Ajersch, F., Ilinca F., Héту, J.-F., Goodwin, F. E., *Iron and Steel Technology*, August (2006): 93-101
- 4) Úředníček, M., Kirkaldy, J.S., *Zeitschrift für Metallkunde*, **64** (1973): 419-427
- 5) Yamaguchi, H., Hisamatsu, Y., *Transactions ISIJ*, **19** (1979): 649-658
- 6) Giannuzzi, L. A., Howell, P. R., Pickering, H. W., Bilster, W. R. in: Galvatech 1992: 461-467
- 7) Leprêtre, Y., Maigne, J. M., Guttmann, M., Philibert, J. in: *Zinc-Based Steel Coating Systems: production and Performance*, Goodwin, F. E. (ed.), (TMS, 1998): 95-107
- 8) Nakano, J., Purdy, G. R., Malakhov, D. V. in: *Summary of XXXI CALPHAD in Stockholm 2002*, Sundman, B. (ed.), *CALPHAD*, **28** (2004): 221-239
- 9) Liu, Y. H., Tang, N.-Y. in: Galvatech 2004: 1155-1164
- 10) Nakano, J., Ph.D. thesis, Department of Materials Science and Engineering, McMaster University, Canada, 2006
- 11) Perrot, P., Tissier, J.-C., Dauphin, J.-Y., *Zeitschrift für Metallkunde*, **83** (1992): 786-790
- 12) Yamaguchi, S., Makino, H., Sakatoku, A., Iguchi, Y. in: Galvatech 1995: 787-794
- 13) Tang, N.-Y., Su, X., *Metallurgical and Materials Transactions A*, **33A** (2002): 1559-1561
- 14) McDermid, J., McMaster University, Canada, private communication, 2005
- 15) Raynor, G. V., Noden, J. D., *Journal of the institute of metals*, **86** (1957): 269-271
- 16) Tang, N.-Y., Su, X., Toguri, J. M., *CALPHAD*, **25** (2001): 267-277
- 17) Yamaguchi, S., University of Tokyo, Japan, private communication, 2005
- 18) Nakano, J., Malakhov, V. D., Purdy, G. R., *CALPHAD*, **29** (2005): 276-288
- 19) H. S. Zurob, J. Nakano, G. R. Purdy, *Journal of Phase Equilibria and Diffusion*, **27** (2006): 699-714
- 20) Purdy, G. R., Malakhov, D. V., Zurob, H. S. in: the 6th international school-conference on phase diagrams in materials science (MSI, 2004): 20-41
- 21) Hillert, M. in: *Lectures on the theory of phase transformations*, Aaronson, H.I. (ed.), (TMS, 1999): 1-33